Article

Internal Heat Exchanger Influence in Operational Cost and Environmental Impact of an Experimental Installation Using Low GWP Refrigerant for HVAC Conditions

Dario Méndez-Méndez [1], Vicente Pérez-García [1,*], Juan M. Belman-Flores [1], José M. Riesco-Ávila [1] and Juan M. Barroso-Maldonado [2]

[1] Department of Mechanical Engineering, Engineering Division, Campus Irapuato-Salamanca, University of Guanajuato, Salamanca 36885, Mexico; d.mendez.mendez@ugto.mx (D.M.-M.); jfbelman@ugto.mx (J.M.B.-F.); riesco@ugto.mx (J.M.R.-Á.)

[2] Engineering College, CETYS University, Mexicali 21259, Mexico; juan.barroso@cetys.mx

* Correspondence: v.perez@ugto.mx; Tel.: +52-46-4647-9940 (ext. 2345)

Abstract: The use of an internal heat exchanger in vapor compression refrigeration systems of one stage is a common practice because it helps to increase the cooling capacity in the evaporator. Furthermore, the use of refrigerants with low global warming potential is becoming more frequent due to environmental regulations worldwide. Thus, this paper presents an evaluation of the improvement produced by the inclusion of an internal heat exchanger cycle (IHXC) in an experimental installation from the viewpoint of exergy, economic and environmental through to exergy, exergoeconomics, and Specific Life Cycle Climate Performance (SLCCP) studies. The tests were conducted using R1234ze(E) as a replacement alternative to R134a in three evaporating temperature conditions: 4 °C, 9 °C, and 14 °C. Comparisons were made considering R134a in BRC mode versus R1234ze(E) in BRC and IHXC modes. Results show that a lower environmental impact is produced by an evaporating temperature of 14 °C with a reduction in SLCCP of 13.3% using IHXC and R1234ze(E). Moreover, the highest increase in exergy efficiency was observed for an evaporating temperature of 4 °C, with this increase being 9%, while the lowest increase in the total cost rate was observed for the same evaporating temperature, being 12.3% and 21.2% for BRC and IHXC modes using R1234ze(E), respectively.

Keywords: IHX; low GWP refrigerants; exergoeconomics; environmental impact; energy

1. Introduction

Recently, the air conditioning and refrigeration industry has evidenced a transition in the use of refrigerants, and one of the main objectives is the replacement of refrigerants that have GWP values higher than three digits. Some measures used to carry out the replacement of refrigerants with high GWP values are found in the current EU regulation 517/2014 (European Union, 2014) [1] and in the Kigali agreement (United Nations, 2016) that have established limitations that require a search for and implementation of new alternative refrigerants in different applications that use vapor compression systems. Among the main objectives of these agreements is the reduction in the use of HFCs worldwide to keep global warming below 1.5 °C to 2 °C; in addition, the Kigali agreement also includes a gradual reduction in the use of HFCs from 2019, which includes developing countries from 2024 and 2028 [2].

The use of HFO in vapor compression systems as low GWP refrigerants has been studied in recent years through theoretical and experimental papers to evaluate energy performance and its thermodynamic characteristics in refrigeration cycles, comparing them with commonly used refrigerants such as R134a. Among them is R1234ze(E), which has attracted attention as a substitute for R134a in certain applications. As a fourth-generation refrigerant, R1234ze(E) satisfies environmental safety requirements for GWP < 10 [3].

Although HFOs have mainly been proposed as substitutes for HFC refrigerants [4], there are some differences in thermophysical properties, which has led to the need to investigate the performance of these alternative refrigerants in systems that have operated with HFCs. To measure the discrepancy, there is a need to search for alternative configurations to the basic vapor compression cycle or to include components that contribute to improving the performance of HFOs.

Based on current information, energy analysis with the use of R1234ze(E) in experimental systems has been widely studied. Mota-Babiloni et al. [5] experimentally evaluated the performance of a water vapor compression system in a direct application of R134a, R1234yf, and R1234ze(E). The authors observed that the use of R1234yf represented a reduction in the cooling capacity of up to 13.71% and a reduction in the COP by up to 10.5%, while the use of R1234ze(E) produced a reduction in the cooling capacity of 33.68% and a lower COP close to 8.4%. Sánchez et al. [6] experimentally compared the HFOs in a direct application in a water-to-water system: R1234ze(E) and R1234yf, among others. For two evaporation temperatures, −10 °C and 0 °C, and three condensation temperatures, 25 °C, 35 °C, and 45 °C, they found that with R1234ze(E), the cooling capacity was reduced between 22.9% and 26.6%, and the reduction in COP was between 2.8% and 13.0%. On the other hand, Devecioglu and Oruç [7] experimentally evaluated the impact of an internal heat exchanger in an air–air vapor compression system using R1234yf and R1234ze(E) as direct substitutes for R134a. They found that the cooling capacity of the system using R134a is higher than that of the system with R1234ze(E); nevertheless, this cooling capacity increased using an internal heat exchanger (IHX) over the basic configuration. Regarding COP, R1234ze(E) presented a better performance compared to R1234yf.

The work carried out by Colombo et al. [8] discussed the results of an experimental study in a water–water heat pump in a drop-in application. They evaluated the performance of R134a and its low GWP alternatives: R1234yf and R1234ze(E). The results reflected that the use of R1234ze(E) represented a substantial reduction in capacity in the range from 14.92% to 33.82%, and a reduction and improvement in the COP in the range of −12.27% to +4.32%. The authors concluded that R1234yf is more suitable for replacing R134a in low- and medium-temperature heat pumps, while R1234ze(E) has better performance for high-temperature heat pumps.

The application in refrigeration systems of R1234ze(E) suggests certain recommendations based on research and experimental tests carried out in various works. In this sense, Mota-Babiloni et al. [4] proposed that the use of this fourth-generation refrigerant should be applied in new refrigerators adapted to the thermophysical characteristics of R1234ze(E), since the experimental results showed that the direct substitution of R1234ze(E) in refrigeration systems designed based on R134a is not suitable, due to the low rates of performance and cooling capacity obtained. One of the applications in which the R1234ze(E) refrigerant is an excellent candidate is in vending machines. For example, Ankit Sethi et al. [9] conducted tests using a larger compressor to obtain a higher cooling capacity related to a higher volumetric displacement provided by the compressor. In general, the changes made to the refrigeration system were minor, including the inclusion of an exchanger in the suction/liquid line with which they managed to match the performance of R134a. Using the higher-capacity compressor, under similar operating conditions, R1234ze(E) presented capacity and efficiency at percentage values of 105% and 90%, respectively. Finally, other papers [10–16] have demonstrated, with energy studies, the use of R1234ze(E) as a feasible alternative to R134a in various applications.

According to the literature, it is evident that R1234ze(E) can be an option as a substitute for R134a in refrigeration applications, mainly considering some retrofit options. Even if the energy study of refrigeration cycles is the most common around the world, there are options such as exergy, exergoeconomics, and environmental studies, which contribute to a wider outlook for evaluating the integral performance of a refrigeration cycle. So, in this paper, the influence of IHX in an experimental installation for HVAC evaporating temperature conditions is analyzed considering not only an energy study but also the

results of exergy, operational cost, and environmental studies, and an integral analysis is carried out that allows us to draw conclusions regarding the viability of R1234ze(E) as an alternative in HVAC applications.

2. Characteristics of R1234ze(E) as an Alternative Refrigerant

In this paper, R1234ze(E) is considered as a replacement alternative to R134a in an experimental installation that operates at medium-high evaporating temperatures. Table 1 shows a comparison of the main characteristics and properties of R1234ze(E) with R134a. The thermodynamic and transport properties have been calculated using REFPROP 10.0® software (NIST—Gaithersburg, MA, USA) [17].

Table 1. Properties of R1234ze(E) and R134a refrigerants.

Property	R134a (HFC)	R1234ze(E) (HFO)
ASHRAE Safety Group	A1	A2L
GWP	1300	<1
ODP	0	0
Critical pressure (kPa)	4059.3	3634.9
Critical temperature (K)	374.2	382.5
Boiling point at 1 atm (K)	247.1	253.9
ASHRAE Flammability	No	Low
ASHRAE Toxicity	No	No
Molecular weight (kg/kmol)	102	114
Liquid density * (kg/m^3)	1294.8	1240.1
Vapor density * (kg/m^3)	14.4	11.7
Specific heat of liquid * (kJ/kgK)	1.34	1.34
Specific heat of vapor * (kJ/kgK)	0.897	0.897
Latent heat of vaporization (kJ/kg)	198.6	184.2
Liquid thermal conductivity * (kJ/kgK)	92×10^{-3}	83.1×10^{-3}
Vapor thermal conductivity * (kJ/kgK)	11.5×10^{-3}	11.6×10^{-3}
Liquid viscosity * (Pa/s)	266.5×10^{-6}	262.6×10^{-6}
Vapor viscosity * (Pa/s)	10.7×10^{-6}	10.7×10^{-6}

* at 273.15 K.

As observed in Table 1, the critical point temperature of R1234ze(E) is higher than that of R134a, which guarantees a higher heat transfer rate when the condenser temperature is far from the critical point temperature [18]. The vapor thermal conductivity of R1234ze(E) is slightly higher than that of R134a, and high values of these properties contribute to improving heat transfer, thereby reducing the initial investment costs related to the purchase of smaller or more compact heat exchangers. Furthermore, the vapor and liquid viscosity of R1234ze(E) are similar and 3% lower, respectively, and these properties are important because low values reduce the energy requirement for its circulation through the system. As for low liquid density values, these can be observed for R1234ze(E), which results in being lower compared to R134a, which represents a lower requirement in the refrigerant charge while also contributing to reducing pressure losses in the connecting lines. Regarding the vapor density, R1234ze(E) presents a lower value; this value is inversely proportional to the gas velocity and the shear force exerted between the vapor and liquid, in which these values are increased and contribute to a positive heat transfer. Several papers have analyzed, in more detail, the thermophysical properties of R1234ze(E) as an alternative in different refrigeration systems [4,19–21].

Environmental Effects

The refrigerants that are the subject of analysis in this paper meet the requirement of not causing damage to the ozone layer considering a zero ODP; however, the GWP represents a real threat that contributes directly to the global warming of the planet. R1234ze(E) has a GWP < 1, considerably lower than the GWP of 1300 presented by R134a. Making

a comparison from the point of view of the GWP, a clear contribution is observed by proposing R1234ze(E) as an alternative to R134a; however, other measurement parameters consider a greater number of factors that contribute to the environmental impact; these are the TEWI (Total Equivalent Warming Impact) and the LCCP (Life-Cycle Climate Performance). The TEWI index is more indicative than the GWP, this represents the impact on global warming due to direct emissions caused by the release of the refrigerant during the useful life of the equipment and the indirect impact due to CO_2 emissions from the use of electrical energy for the operation of the system. Lastly, the LCCP considers, in addition to direct emissions, the emissions caused indirectly by using each fluid and the refrigeration system, while also considering all the relevant indirect emissions involved in the life cycle of the refrigerant compared to the TEWI, such as emissions related to the manufacture and disposal of this, as well as the life use of the system. This is how, in this paper, the LCCP analysis of the environmental impact generated by operating refrigerants R134a and R1234ze(E) under the proposed operating conditions is carried out. Here we seek to observe the influence represented by the low GWP of R1234ze(E) and the refrigerant charge of the system for each configuration, as well as the impact on indirect emissions due to energy consumption and the inclusion of the IHX for each refrigerant based on its thermal performance for each cycle.

3. Experimental Procedure

For the development of the experimental tests, a vapor compression installation is available, which integrates three systems: The refrigeration circuit (Figure 1a) and two secondary circuits, the load simulator (Figure 1b) and the heat sink (Figure 1c).

Figure 2 illustrates the experimental configuration used to study the behavior of the refrigerants in the refrigeration installation. This diagram contains all the main components of the installation, sensors, and instrumentation, in addition to the equipment that makes up the secondary circuits responsible for simulating and dissipating the thermal load within the vapor compression cycle, all for the correct operation of the configuration. The fluid used by the thermal load simulator circuit consists of a water–glycol mixture with a 70/30 volume percentage, while the thermal load dissipation circuit uses saturated water as the working fluid. Temperature and pressure sensors were used, which were located at the inlet and outlet of each component. The main characteristics of the sensors, flowmeters, and power meters are shown in Table 2.

Table 2. Specifications of the elements and devices for measuring temperature, pressure, flow, and electrical power.

Sensor	Specification	Measuring Range	Sensitivity
Temperature	Thermocouple type K	−270 to 1372 °C	3.6 mV/100 °C
Pressure	WIKA	0 to 25 bar and 0 to 100 bar	$\leq \pm 0.3\%$
Coriolis flowmeter	SITRANS FC Coriolis	4500 kg/h	$\pm 0.2\%$ with liquids and $\pm 0.4\%$ with gases
Electromagnetic flowmeter (Secondary circuits)	ONICON	0.1 to 0.6 kg/s	$\pm 0.4\%$
Power measurement	FLUKE 1736	1000 V and 40 A	$\pm 0.2\%$ V and $\pm 0.7\%$ A

The vapor compression circuit of the refrigeration installation consists of the following components: A hermetic reciprocating compressor of 2.6 m^3/h of displacement volume, two plate heat exchangers that act as condenser and evaporator of 3.5 kW and 2.5 kW capacity, respectively, a 3-L capacity liquid receiver, and a 5.0 kW nominal capacity thermostatic expansion valve. Finally, an internal heat exchanger was added, which is a plate and has a capacity of 2.5 kW. All plate heat exchangers are arranged to operate in countercurrent. Table 3 shows the main characteristics of the heat exchangers that are part of the experimental installation.
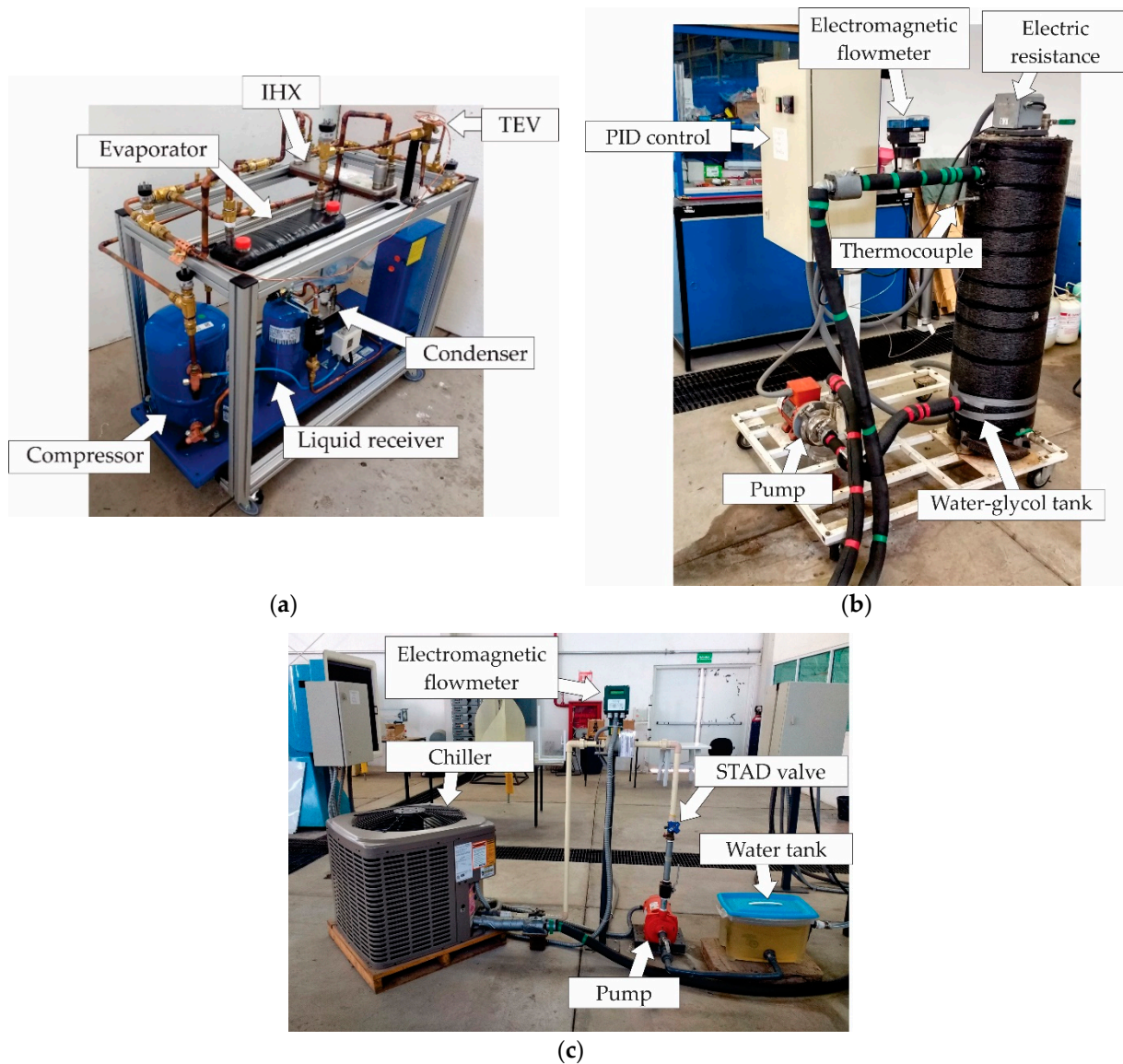
(**a**)

(**b**)

(**c**)

Figure 1. Experimental installation: (**a**) Refrigeration circuit, (**b**) thermal load simulator, and (**c**) thermal load sink.

Table 3. Specifications of the heat exchangers of the experimental installation.

Component	Specification	Number of Plates	Dimensions (cm) (Length × Width × Height)
Evaporator	PHE B3-030-10	10	32.5 × 9.5 × 2.4
Condenser	PHE B3-030-20	20	32.5 × 9.5 × 3.9
IHX	PHE B3-030-10	10	32.5 × 9.5 × 2.4

A vapor compression refrigeration installation was available to carry out the experimental tests, which can operate two configurations of the vapor compression cycle:
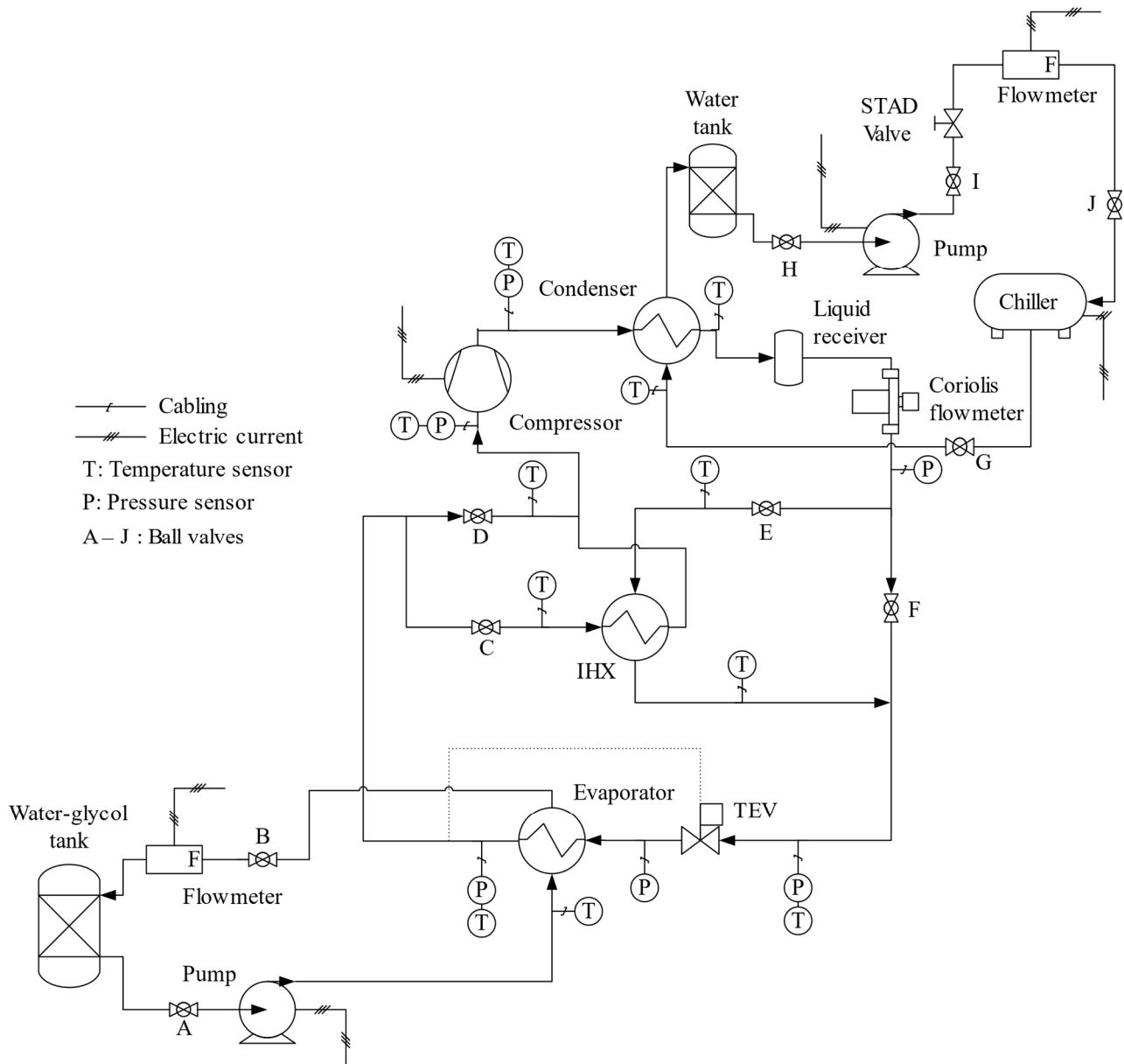
- BRC.
- IHXC.

Figure 2. Schematic representation of the experimental setup.

3.1. Basic Refrigeration Cycle (BRC)

Figure 3a represents the conventional vapor compression refrigeration cycle, where the liquid refrigerant evaporates in the low-pressure stage (4-1), is compressed (1-2), and is condensed in the high-pressure stage (2-3). Subsequently, the refrigerant leaves subcooled (4) and then passes through the expansion device, in this case, a thermostatic expansion valve (TEV) (3-4), which decreases the temperature and pressure of the refrigerant to enter the evaporator with a certain quality, where the refrigerant evaporates, absorbing the heat of the fluid that is required to cool; once the refrigerant leaves the evaporator, it passes through the suction of the compressor (1) to repeat the cycle. Figure 3b show this configuration, which is composed of a compressor, condenser, liquid receiver, thermostatic expansion valve, and evaporator.
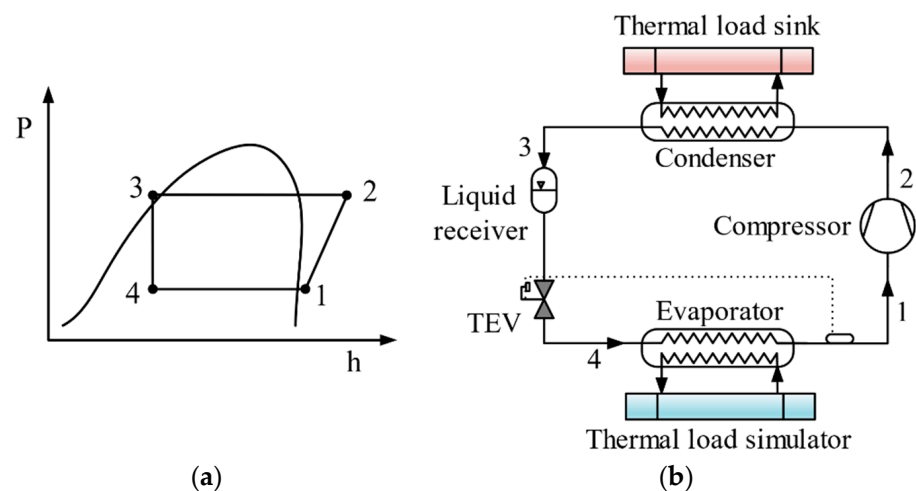
Figure 3. (**a**) P-h diagram of basic refrigeration cycle, (**b**) scheme of basic refrigeration cycle (BRC) in experimental installation.

3.2. Use of an IHX as Improvement on BRC

The IHX or suction/liquid line heat exchanger promotes heat exchange between the refrigerant at the condenser outlet (3-4) and the evaporator outlet (6-1), in such a way that a sufficient degree of subcooling (SUB) is guaranteed at the condenser outlet, influencing the decrease in the quality of the refrigerant at the evaporator inlet and increasing the latent heat portion. Therefore, this component promotes an increase in the cooling capacity in the evaporator as a result of the increase in the enthalpy jump in the evaporation phase. Similarly, IHX produces an increase in the temperature of the refrigerant at the outlet of the evaporator, an effect known as superheating (SUP). Both effects can be seen in Figure 4a. In Figure 4b, the inclusion of IHX is shown as a modification of the basic refrigeration cycle, and in this paper, this modification is called IHXC.
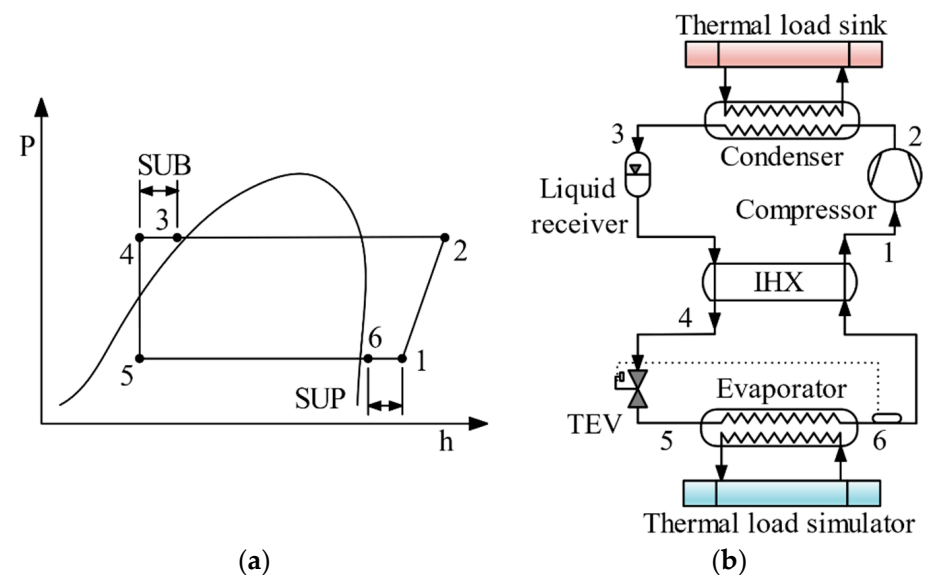

Figure 4. (**a**) P-h diagram of IHXC, (**b**) scheme of IHXC.

4. Integral Analysis

An integral analysis allows for evaluating a scenario from different edges. In this paper, the integral analysis of refrigerants was performed considering energy, exergy, exergoeconomics, and environmental studies, which are described in the following subsections.

4.1. Energy Study

For the development of the energy study, both the cooling capacity and the coefficient of performance (COP) were considered, since these parameters provide direct information on the capacity of the refrigerants used to remove the thermal load set as a function of its thermophysical properties. In the same way, they present the relationship between the cooling capacity and the energy consumption in the cycle for each of the analyzed fluids. The cooling capacity is obtained by multiplying the mass flow of the refrigerant by the increase in enthalpy in the evaporator (1). The mass flow of the refrigerant is of great importance in the calculation of the cooling capacity since it allows one to determine the speed at which the energy transfer occurs in the system.

$$\dot{Q}_{evap} = \dot{m}_{ref}(h_{out} - h_{in})_{evap} \tag{1}$$

For the calculation of the COP (2), the cooling capacity occurring in the evaporator and the ratio at which the work is required in the compressor are considered.

$$COP = \frac{\dot{Q}_{evap}}{\dot{W}_{comp}} \tag{2}$$

Table 4 summarizes the equations used in the analysis of each of the installation components considered for the calculation of the cycle performance parameters.

4.2. Exergy Study

Through the analysis of the irreversibility of the system, the number of thermodynamic inefficiencies in each of the components and of the system, in general, are identified [22–24]. The exergy destroyed, calculated when the exergy balance is carried out in each component, refers to losses in the quality of energy in the system, which would be very difficult to determine through an energy analysis [25].

In vapor compression refrigeration systems, the physical exergy consists of the maximum useful work that is obtained when passing from an initial state (T, P) to a reference state (T_o, P_o). In this case, chemical, magnetic, electrical, and nuclear exergy are neglected. The physical exergy of a flow stream can be expressed as:

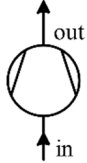$$\dot{E}^{PH} = \dot{m}_{ref} \cdot e^{PH} = \dot{m}_{ref}[(h - h_o) - T_o(s - s_o)] \tag{3}$$
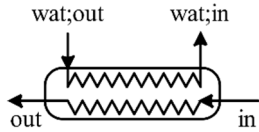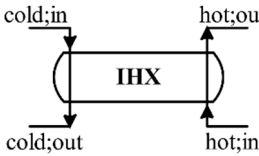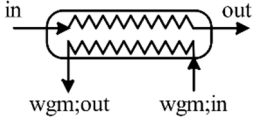
The exergy balance for installation components is summarized in Table 4. The total exergy destruction ratio consists of the sum of the exergy destruction of each component, expressed as:

$$\dot{E}_{D;TOT} = \dot{E}_{D;comp} + \dot{E}_{D;cond} + \dot{E}_{D;TEV} + \dot{E}_{D;evap} + \dot{E}_{D;IHX} \tag{4}$$

Based on the second law of thermodynamics, the performance criterion for the entire refrigeration system is the rational efficiency, which consists of the difference between a unit and the fraction of the total exergy destruction ($\dot{E}_{D;TOT}$) and the power consumption in the compressor ($\dot{W}_{comp}$), which can be written as [24]:

$$\psi = 1 - \frac{\dot{E}_{D;TOT}}{\dot{W}_{comp}} \tag{5}$$

Table 4. Characteristic equations of each component of the installation.

Component	Model	Energy Analysis	Exergy Analysis	Exergoeconomic Analysis
Compressor		$n_{iso} = \frac{h_{out;iso} - h_{in}}{h_{out} - h_{in}}$ $\dot{W}_{comp} = \dot{m}_{ref}(h_{out} - h_{in})_{comp}$	$\dot{W}_{comp} - \left(\dot{E}_{out} - \dot{E}_{in}\right) = \dot{E}_{D;comp}$	$\dot{C}_{out} = \dot{C}_{in} + \dot{C}_{w;comp} + \dot{Z}_{comp}$
Condenser		$\dot{Q}_{cond} = \dot{m}_{ref}(h_{in} - h_{out})_{cond}$	$\left(\dot{E}_{in} - \dot{E}_{out}\right) - \left(\dot{E}_{wat;out} - \dot{E}_{wat;in}\right) = \dot{E}_{D;cond}$	$\dot{C}_{wat;out} + \dot{C}_{out} = \dot{C}_{in} + \dot{C}_{wat;in} + \dot{Z}_{cond}$
IHX		$\varepsilon = \frac{T_{cold;out} - T_{cold;in}}{T_{hot;in} - T_{cold;in}}$	$\left(\dot{E}_{hot;in} - \dot{E}_{hot;out}\right) - \left(\dot{E}_{cold;out} - \dot{E}_{cold;in}\right) = \dot{E}_{D;IHX}$	$\dot{C}_{cold;out} + \dot{C}_{hot;out} = \dot{C}_{cold;in} + \dot{C}_{hot;in} + \dot{Z}_{IHX}$
TEV		$h_{in} = h_{out}$	$\dot{E}_{in} - \dot{E}_{out} = \dot{E}_{D;TEV}$	$\dot{C}_{out} = \dot{C}_{in} + \dot{Z}_{TEV}$
Evaporator		$\dot{Q}_{evap} = \dot{m}_{ref}(h_{out} - h_{in})_{evap}$	$\left(\dot{E}_{wgm;in} - \dot{E}_{wgm;out}\right) - \left(\dot{E}_{out} - \dot{E}_{in}\right) = \dot{E}_{D;evap}$	$\dot{C}_{out} + \dot{C}_{wgm;out} = \dot{C}_{in} + \dot{C}_{wgm;in} + \dot{Z}_{evap}$

4.3. Exergoeconomic Study

The exergoeconomic or thermoeconomic analyses known in the literature relate to the costs associated with the exergy currents for each component of the system, in addition to the capital costs of the equipment in monetary units. The equation that reflects the balance of the economic cost based on the exergy of the system is expressed as:

$$\sum_{in} \dot{C}_k + \dot{Z}_{TOT} = \sum_{out} \dot{C}_k \tag{6}$$

where the cost terms are evaluated as (7); here (c_k) represents the unit exergy cost and ($\dot{E}_k$) is the exergy rate.

$$\dot{C}_k = c_k \times \dot{E}_k \tag{7}$$

For each component, the economic cost balance based on the input exergy (F: Fuel) and product exergy (P: Product) is expressed as (8).

$$\dot{C}_P = \dot{C}_F + \dot{Z}_K \tag{8}$$

The total levelized hourly cost of each component is calculated as:

$$\dot{Z}_k^{TOT} = \dot{Z}_k^{CI} + \dot{Z}_k^{OM} \tag{9}$$

where $\dot{Z}_k^{CI}$ and $\dot{Z}_k^{OM}$ are the cost of capital investment and the cost of operation and maintenance, evaluated per year, respectively. In Mexico, the investment costs in dollars for each component of the installation are shown in Table 5.

Table 5. Capital investment cost of each component.

Component	Capital Investment Cost ($)
Compressor	751.11
Condenser	144.52
TEV	34.16
Evaporator	98.37
IHX	98.37

For the calculation of these two parameters, the capital recovery factor (CRF) is introduced to consider the interest rate and the operating time of the system.

$$CRF = \frac{i_r(i_r+1)^n}{(i_r+1)^n - 1} \tag{10}$$

$$\dot{Z}_k^{CI} = \frac{cRF}{t_{ope}} \cdot Z_k \tag{11}$$

$$\dot{Z}_k^{OM} = \dot{Z}_k^{CI} \cdot \varphi \tag{12}$$

Information about certain factors for the evaluation of the previous equations is shown in Table 6.

To determine the exergoeconomic performance of the two configurations of the installation, the exergy and exergoeconomic balance equations are used, which are listed in Table 4.

To evaluate the exergoeconomic performance of the specific system, the following parameters are defined:

The cost rate is associated with the exergy destructions, which takes into account the unitary exergy cost of the current it makes as fuel for the component ($c_{F,k}$) and the exergy destruction ratio ($\dot{E}_{D,k}$),

$$\dot{C}_{D,k} = c_{F,k} \times \dot{E}_{D,k} \tag{13}$$

Table 6. The assumed parameters for the exergoeconomic analysis.

Parameter	Description	Unit	Value
i_r	Interest rate [1]	%	10
n	Lifetime	year	15
t_{ope}	Annual operating time	h	4000
φ	Operation and maintenance cost factor [2]	%	1.06

[1] was placed based on ref. [26]; [2] was placed based on ref. [27].

The total exergy cost rate is the sum of the cost ratio associated with exergy destruction ($\dot{C}_{D,k}$) and the total levelized hourly cost of each component ($\dot{Z}_k^{TOT}$).

$$\dot{C}_{TOT,k} = \dot{C}_{D,k} + \dot{Z}_k^{TOT} \tag{14}$$

4.4. Life Cycle Climate Performance Study

The LCCP analysis is a holistic measurement method that takes into account the impact of the use of a refrigeration system with a certain refrigerant during its useful life. It is more complex than the TEWI, but it considers more factors that influence the measurement of the environmental impact [28]. The methodology for calculating the LCCP described below was investigated from the available literature [29]. The LCCP is the sum of the direct and indirect emissions in the operation of a refrigeration system, and it is based on (15) and is measured in $kgCO_{2eq}$ or the SLCCP in $kgCO_{2eq}/kWh$.

$$LCCP = \text{Direct emissions} + \text{Indirect emissions} \tag{15}$$

Direct emissions refer to the environmental impact produced by refrigerant leaks once it is charged to the installation, and its calculation is conducted with (18).

$$DE = C \times (L \times ALR + EOL) \times (GWP + adp\,.GWP) \tag{16}$$

where C is the refrigerant charge (kg), L is the average equipment life (years), ALR is an annual leak rate (% of refrigerant charge), EOL is the end-of-life refrigerant leak useful (% of refrigerant charge), GWP is the global warming potential ($kgCO_{2eq}/kg$), and adp.GWP is the GWP of the atmospheric degradation product of the refrigerant ($kgCO_{2eq}/kg$).

Indirect emissions include emissions from energy consumption, the manufacturing of materials, the manufacturing of the refrigerant, and the disposal of the unit (17).

$$\begin{aligned} IE = {} & \text{Energy consumption} + \text{Equipment manufacturing} + \text{Equipment EOL} \\ & + \text{Refrigerant manufacturing} \end{aligned} \tag{17}$$

Emissions from energy consumption are calculated by (18).

$$\text{Energy Consumption Emissions} = L \times AEC \times EM \tag{18}$$

where AEC represents the annual energy consumption (kWh/year) and EM is the emission factor of the power plant ($kgCO_{2eq}/kWh$). EM is calculated from the share of resources for power plants in the electricity generation region.

The other indirect emission factors are calculated from (19)–(21).

$$\text{Equipment manufacturing} = \sum(MM \times m) \tag{19}$$

$$\text{Equipment EOL} = \sum(\text{RM} \times \text{Mr}) \tag{20}$$

$$\text{Refrigerant manufacturing} = (C + C \times \text{ALR} \times L) \times \text{RFM} + \text{RFD} \tag{21}$$

where MM is the CO_{2eq} produced/kg of material ($kgCO_{2eq}$/kg), m is the mass of the unit/material (kg), RM is the CO_{2eq} produced/kg of recycled material ($kgCO_{2eq}$/kg), Mr is the mass of recycled material (kg), RFM represents the emissions from the manufacture of the refrigerant ($kgCO_{2eq}$/kg), and RFD represents the emissions from the disposal of the refrigerant ($kgCO_{2eq}$/kg).

The information regarding the parameters to evaluate the previous equations required in the LCCP analysis is shown in Table 7. Some factors are taken from information in the available literature, due to the complexity of determining them.

Table 7. Input parameters for LCCP analysis.

Item	R134a BRC	R1234ze(E) BRC	R1234ze(E) IHXC
Refrigerant charge, kg	0.52	0.5	0.63
Unit weight, kg	115	115	120
Annual refrigerant leakage [1,2], %	4	4	4.4
EOL leakage [1,2], %	15	15	17
Lifetime [1], year	15	15	15
Equipment manufacturing [3], $kgCO_{2eq}$	409	409	450
Nominal cooling capacity, kW	3.0	3.0	3.5

[1] was placed based on ref. [30]; [2] was placed based on ref. [31]; [3] was placed based on ref. [32].

5. Results

5.1. Cooling Capacity

To determine the cooling capacity, the thermodynamic states at the inlet and outlet of each component were defined experimentally. Table 8 shows a summary of the operating pressures of each cycle and the overheating at the outlet of the evaporator provided by the TEV for the configurations analyzed in the experimental installation.

Table 8. Experimental thermal operating conditions for each installation cycle configuration.

Refrigerant	Configuration	Evaporation Temperature (°C)	Suction Pressure (kPa)	Discharge Pressure (kPa)	Superheating (K)
R1234ze(E)	BRC	4	152.2	672.3	4.89
		9	189.9	679.2	5.14
		14	254.3	686.5	5.39
R1234ze(E)	IHXC	4	165.7	680.2	5.28
		9	202.4	696.4	5.09
		14	267.1	701.1	5.37
R134a	BRC	4	226.1	883.8	5.54
		9	299.2	893.6	5.92
		14	370.9	911.1	5.43

Figure 5 represents the cooling capacity varying the evaporation temperature when the installation is operated in both BRC and IHXC. To obtain the three evaporation temperature conditions, the inlet temperature of the water–glycol mixture in the evaporator was varied for three controllable values of 10, 15, and 20 °C, which guaranteed the approximate evaporation temperatures of 4, 9, and 14 °C of the refrigerant. Similarly, Figure 4 shows the influence of the volumetric flow condition of the mixture ($C_{min;mix}$ = 0.141 L/s and $C_{max;mix}$ = 0.162 L/s). In this case, when operating the IHXC, it was found that due to the sub-cooling at the condenser outlet caused by the IHX, the enthalpy at the evaporator inlet is reduced, and the smaller this value, the higher the

increase in the cooling capacity. Likewise, when the evaporation temperature increases, the cooling capacity also increases. It is also highlighted that for the R1234ze(E) to match the cooling capacity obtained by the R134a in the BRC, it is necessary to implement the IHXC to match this performance parameter.
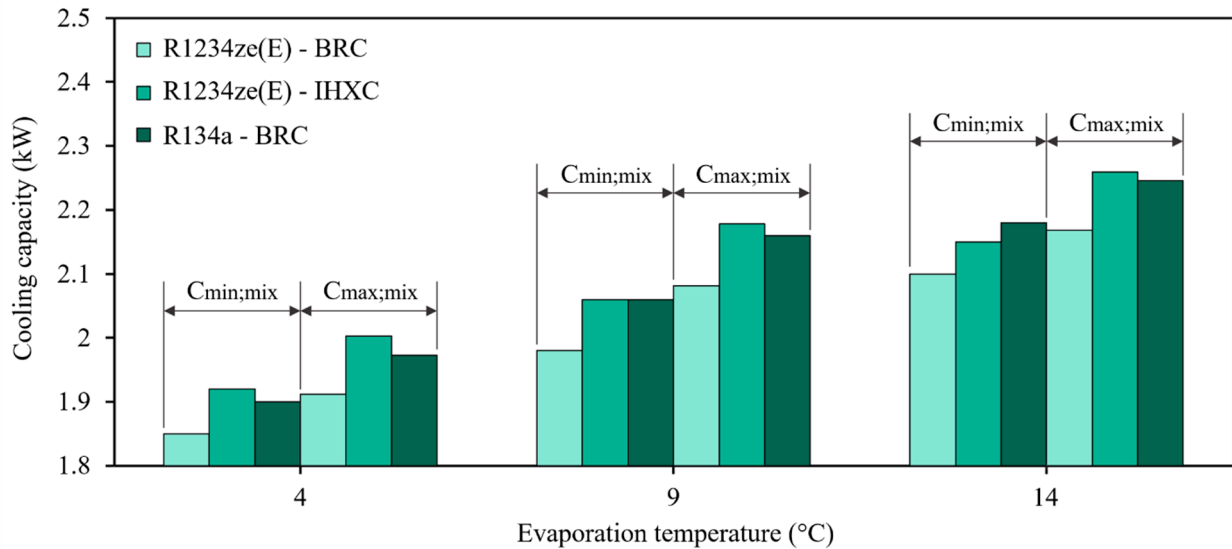

Figure 5. Variation of the cooling capacity for the two flow conditions of the water–glycol mixture.

Considering the maximum flow condition in the water–glycol mixture ($C_{max;mix}$ = 0.162 L/s), an increase is observed in the cooling capacity for the cycles operated in a range of 3.1% to 5.6% regarding the results obtained with the minimum flow condition of the mixture, which suggests that the increase in volumetric flow improves the energy transfer in the evaporator. Similarly, for this flow condition, the inclusion of the IHX is necessary so that the cooling capacity of R1234ze(E) reaches that of R134a operating in the BRC. Considering properties that influence the improvement of the cooling capacity is the thermal conductivity of liquid and vapor, and R1234ze(E) has a lower thermal conductivity of liquid compared to R134a, presenting lower values in this performance parameter; however, in the case of vapor thermal conductivity, it is slightly higher for R1234ze(E), and with the help of IHX, it is possible to match the cooling capacity.

5.2. Coefficient of Performance (COP)

The results obtained regarding the COP for the two refrigerants and the two cycles handled in the installation are shown in Table 9, which reflects the variation of the COP for the three evaporation conditions. Moreover, considering the maximum flow rate of the water–glycol mixture ($C_{max;mix}$ = 0.162 L/s), the flow condition for which a higher cycle performance is obtained without requiring a large difference in flow power in the thermal load simulator circuit concerning that used for the minimum flow condition. The favorable effect of the subcooling caused by activating the IHX within the cycle can be appreciated, producing an increase in the cooling capacity in the evaporator. In the same way, increasing the evaporation temperature produces a lower requirement in the compression work, thus contributing to the increase in the COP. When comparing R1234ze(E) and R134a operating the BRC, there is a reduction in the COP between 3.3% and 5.5%, and when including the IHX using R1234ze(E), these differences are reduced by between 0.32% and 1.5%. Similarly, by incorporating the IHX and presenting a lower liquid density with respect to R134a, a reduction in the refrigerant charge required for the two cycle configurations is observed, with which a lower flow power is needed, thus improving the COP.

Table 9. Results of the performance parameters of each refrigerant for the two operating cycles of the installation.

| Refrigerant	Configuration	Evaporation Temperature Operational (°C)	Compression Power (kW)	COP	ψ (%)	TCR ($/h)	SLCCP (kgCO$_{2eq}$/kWh)
R134a	BRC	4	0.883	3.165	29.96	0.07667	63.64
		9	0.835	3.544	34.65	0.06228	59.45
		14	0.798	3.871	38.69	0.05403	57.46
	IHXC	4	0.859	3.306	38.67	0.08784	62.35
		9	0.823	3.622	40.28	0.07145	59.72
		14	0.779	4.049	42.99	0.07148	60.11
R1234ze(E)	BRC	4	0.909	3.064	28.17	0.08744	58.83
		9	0.867	3.359	29.52	0.07406	59.87
		14	0.841	3.726	33.80	0.06405	54.72
	IHXC	4	0.872	3.155	32.95	0.09726	57.32
		9	0.824	3.493	35.19	0.09093	54.47
		14	0.793	3.849	36.88	0.08053	50.7

5.3. Exergy Efficiency

The exergy efficiency for each refrigerant is reflected in Table 9. R134a offers a better exergy performance of between 6.3 and 17.4% compared to R1234ze(E) in BRC mode, because R134a has a greater cooling capacity in the evaporator that influences the reduction of the total irreversibility for that refrigerant, and properties such as the higher thermal conductivity of R134a favor these results. It can also be seen that the inclusion of IHX for both refrigerants contributes to an increase in exergy efficiency; this improvement is offset by the contribution to the irreversibility implied by the inclusion of this new component in the BRC. In general, the improvement in exergy performance with the inclusion of IHX represented an increase of between 8.3 and 16.1% for R1234ze(E). In addition, if IHXC is compared with R1234ze(E), it can match the exergy performance that BRC represents with R134a, even for a temperature of 4 °C in evaporation, and it can improve the exergy efficiency by 9%.

5.4. Destruction of Exergy

Figure 6 shows the exergy destruction for each component of the installation for the maximum flow condition of the water–glycol mixture in the two cycle configurations for each refrigerant. The exergy destruction values for each of the components of the two cycles manipulated in the installation using R1234ze(E) are similar to those obtained for R134a since, by increasing the evaporation temperature and the total irreversibilities of the system, comparing the two cycles for R1234ze(E), when manipulating the IHXC, a decrease between 4% and 9.4% was observed for the range of evaporation temperatures. Considering the exergy destruction for each component, in the case of R1234ze(E), the exergy destruction was higher compared to R134a; however, the inclusion of IHX positively influenced a maximum reduction of 28.3% in the irreversibility of the TEV and 20.1% in the compressor, present in the BRC. The compressor is the component that presents the highest exergy destruction ratio for each cycle configuration, due to the high-pressure ratio values that lead to a higher compression power requirement for all the conditions evaluated.
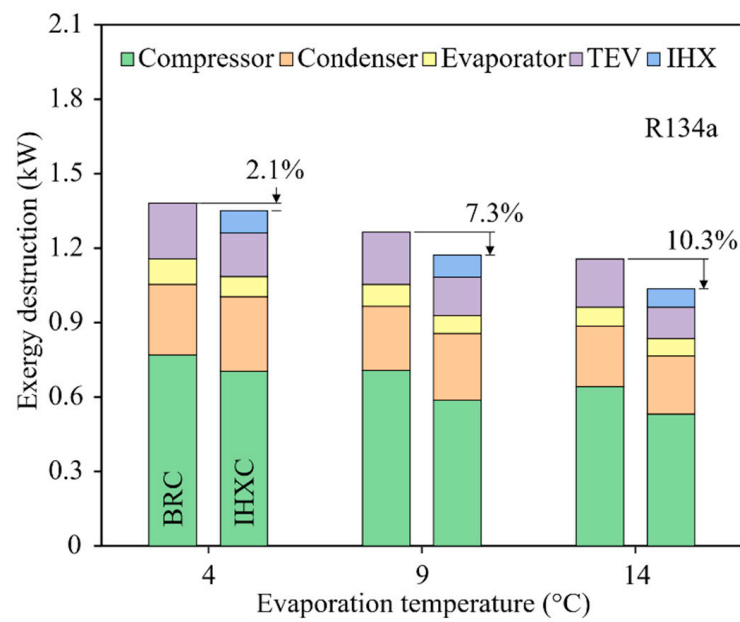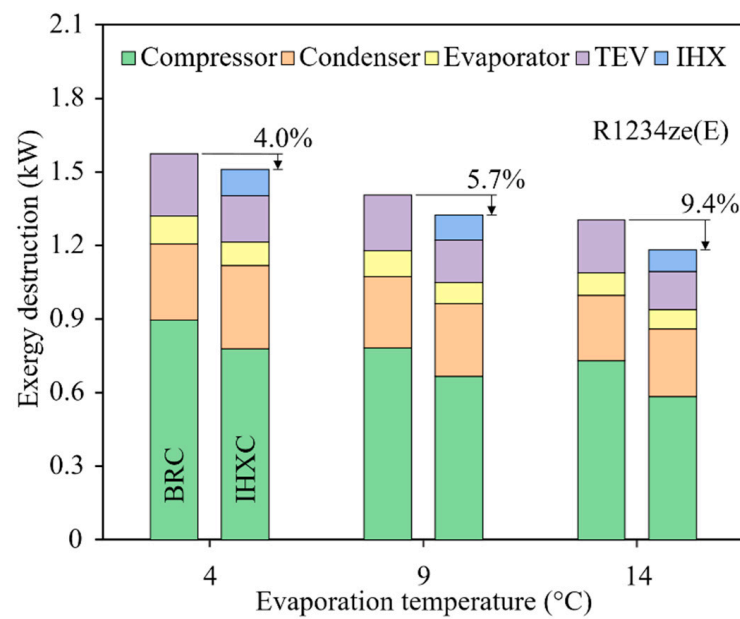
Figure 6. Destruction of exergy in each component of the BRC and IHXC using (**a**) R134a, (**b**) R1234ze(E).

5.5. Operational Costs

The total operating cost, which considers the exergy destruction value of the system, the capital investment, and the cost of electrical energy consumption for the operation of each of the cycle configurations, is shown in Table 9. The exergy destruction costs of each component for the two configurations have an important influence. R1234ze(E) has a lower exergy performance than R134a and, therefore, higher exergy destruction costs that cause an increase in the total operating cost of the system. The differences in operating costs between the two refrigerants considering the BRC are between 14.0% and 18.9% and for IHXC vary between 10.7% and 27.3%.

5.6. LCCP Evaluation

LCCP is a complete tool due to the fact it considers energy embodied in product materials, greenhouse gas emissions during chemical manufacturing, and the end-of-life disposal of the unit. In this sense, the LCCP method should be used when a more in-depth analysis of the environmental impact of a unit is warranted. From Table 9, a comparison of the total amount of emissions of $kgCO_{2eq}$ for each of the refrigerants is analyzed using specific LCCP (SLCCP), which was calculated by dividing total emissions by the amount of kWh consumed by the unit. Due to the high GWP of R134a, it is noted that it influences the impact of direct emissions when operating with this refrigerant. The improvement in total direct emissions when using R1234ze(E) compared to R134a is close to 100%. Another very useful aspect that Table 9 provides is the great influence of the energy consumption factor. Even though operation with R1234ze(E) implied a minimum reduction in energy consumption of approximately 3%, reducing this factor for the operation of the system implies an opportunity for improvement of the cycle, focused both on the thermal performance and the substantial reduction in the negative impact on the environment. This could be addressed by using a new configuration or modification of the compression cycle, in such a way that the energy consumption of the system can be reduced. Considering the total emissions of $kgCO_{2eq}$ per kWh required to operate the system, a reduction in this specific climate performance parameter is presented when using R1234ze(E) relative to R134a. When the BRC is operated, the reduction is between 0.7% and 8.2%, and for the IHXC configuration, the reduction varies between 8.8% and 18.5% for the evaporation conditions considered.

6. Conclusions

In this paper, the experimental analysis of the energy performance and the environmental impact of R1234ze(E) as an alternative to R134a has been investigated in a refrigeration installation under medium-high evaporation temperature conditions. COP and cooling capacity were the parameters used to evaluate energy performance, exergy efficiency and the total cost rate represent the exergy and exergoeconomic performance, and finally, an SLCCP analysis was performed to measure the emissions in $kgCO_{2eq}$ for the two refrigerants. The highlighted conclusions are summarized below.

The IHX contribution for R1234ze(E) concerning BRC translates into an increase between 4% and 4.5% in cooling capacity, and for COP, an increase between 2.9% and 3.8%; however, for the two flow conditions of the water–glycol mixture, it is necessary to incorporate the IHX when working with R1234ze(E) to match the cooling capacity and the COP of the R134a in the BRC.

The inclusion of IHX can improve the exergy performance for the evaporation conditions considered by up to 9% concerning the BRC and is likely to have a great positive impact, in the case of the R1234ze(E) reducing the irreversibility of the compressor and the TEV.

With R1234ze(E), it is possible to reduce the refrigerant charge for the evaluated cycle configurations because it presents lower density values compared to R134a. This produces a reduction in the energy consumption of the system, and considering the environmental aspect, the LCCP decreases.

The LCCP analysis showed that R1234ze(E) represents a reduction in total emissions of $kgCO_{2eq}$ by 10.7% compared to R134a. Direct emissions and energy consumption are the major contributors to the LCCP, establishing an opportunity for improvement for future research. The SLCCP of R1234ze(E) in IHXC mode compared to BRC and R134a showed a reduction of between 9.1% and 13.3% for the evaporation range considered.

According to the results, R1234ze(E) is a suitable alternative to R134a for medium-high evaporation temperature conditions common in applications such as vending machines, water chillers, and commercial refrigeration, among others, considering the inclusion of IHX, which does not represent a large investment.

Nomenclature

A	amps
C	flow, L/s
c	unit exergy cost, $/kJ
$\dot{C}$	exergy cost rate, $/h
Ch	refrigerant charge, kg
DE	direct emissions, $kgCO_{2eq}$
$\dot{E}$	exergy rate, kW
EM	power plant emission factor, $kgCO_{2eq}$/kWh
h	specific enthalpy, kJ/kg
IE	indirect emissions, $kgCO_{2eq}$
i_r	interest rate, %
L	average lifetime of equipment, year
$\dot{m}$	mass flow rate, kg/s
M	mass of unit or material, kg
MM	CO_{2e} produced per kg of material, $kgCO_{2eq}$/kg
Mr	mass of recycled material, kg
n	lifetime, year
P	pressure, kPa
$\dot{Q}$	heat transfer, kW
s	specific entropy, kJ/kg-K
t_{ope}	annual operating time, h
T	temperature, °C
V	volts
$\dot{W}$	power consumption, kW
Z	purchase cost associated with a component, $
$\dot{Z}$	capital cost rate, $/h

Abbreviations

Adp.GWP	GWP of atmospheric degradation product of the refrigerant: $kgCO_{2eq}$/kg
AEC	annual energy consumption, kWh
ALR	annual leakage rate, % of refrigerant charge
BRC	basic refrigeration cycle
COP	coefficient of performance
CRF	capital recovery factor
EOL	end of life refrigerant leakage, % of refrigerant charge
GWP	global warming potential
HFC	hydrofluorocarbon
HFO	hydrofluoroolefin
IHXC	cycle with internal heat exchanger
IIR	institute of international refrigeration

LCCP	life cycle climate performance
ODP	ozone depletion potential
RFD	refrigerant disposal emissions per unit mass of refrigerant, $kgCO_{2eq}/kg$
RFM	refrigerant manufacturing emissions per unit mass of refrigerant, $kgCO_{2eq}/kg$
SLCCP	specific life cycle climate performance, $kgCO_{2eq}/kWh$
SUB	subcooling
SUP	superheating
TCR	total cost rate, \$/h
TEV	thermostatic expansion valve

Subscripts

CI	capital investment
cold	cold stream
comp	compressor
cond	condenser
D	destruction
eq	equivalent
evap	evaporator
f	fuel
hot	hot stream
in	inlet
iso	isentropic
k	component
max	maximum
min	minimum
mix	mixture
o	ambient
OM	operation and maintenance
out	outlet
p	product
PH	physical
ref	refrigerant
TOT	total
wat	water
wgm	water-glycol mixture

Greek symbols

ε	effectiveness
ϵ	efficiency
φ	operation and maintenance cost factor
ψ	rational efficiency

References

1. European Commission. Regulation (EU) No 517/2014 of the European Parliament and the Council of 16 April 2014 on fluorinated greenhouse gases and repealing Regulation (EC) No 842/2006. *Off. J. Eur. Union* **2014**, *L150*, 195.
2. UNEP (United Nations Environment Programme). Twenty-Eighth Meeting of the Parties to the Montreal Protocol on Substances that Deplete the Ozone Layer. *Furth. Amend. Montr. Protoc.* **2016**, 1–72. Available online: https://ozone.unep.org/sites/default/files/2019-08/MOP-28-12E.pdf (accessed on 20 March 2022).
3. Liu, W.; Meinel, D.; Wieland, C.; Spliethoff, H. Investigation of hydrofluoroolefins as potential working fluids in organic Rankine cycle for geothermal power generation. *Energy* **2014**, *67*, 106–116. [CrossRef]
4. Mota-Babiloni, A.; Navarro-Esbrí, J.; Molés, F.; Cervera, Á.B.; Peris, B.; Verdú, G. A review of refrigerant R1234ze(E) recent investigations. *Appl. Therm. Eng.* **2016**, *95*, 211–222. [CrossRef]
5. Mota-Babiloni, A.; Navarro-Esbrí, J.; Barragán, Á.; Molés, F.; Peris, B. Drop-in energy performance evaluation of R1234yf and R1234ze(E) in a vapor compression system as R134a replacements. *Appl. Therm. Eng.* **2014**, *71*, 259–265. [CrossRef]
6. Sánchez, D.; Cabello, R.; Llopis, R.; Arauzo, I.; Catalán-Gil, J.; Torrella, E. Energy performance evaluation of R1234yf, R1234ze(E), R600a, R290 and R152a as low-GWP R134a alternatives. *Int. J. Refrig.* **2017**, *74*, 269–282. [CrossRef]
7. Devecioglu, A.G.; Oruc, V. Improvement on the energy performance of a refrigeration system adapting a platetype heat exchanger and low-GWP refrigerants as alternatives to R134a. *Energy* **2018**, *155*, 105–116. [CrossRef]
8. Colombo, L.P.M.; Lucchini, A.; Molinaroli, L. Experimental analysis of the use of R1234yf and R1234ze(E) as drop-in alternatives of R134a in a water-to-water heat pump. *Int. J. Refrig.* **2020**, *115*, 18–27. [CrossRef]

9. Sethi, A.; Vera Becerra, E.; Yana Motta, S. Low GWP R134a replacements for small refrigeration (plug-in) applications. *Int. J. Refrig.* **2016**, *66*, 64–72. [CrossRef]

10. Nawaz, K.; Shen, B.; Elatar, A.; Baxter, V.; Abdelaziz, O. R-1234yf and R-1234ze(E) as low-GWP refrigerants for residential heat pump water heaters. *Int. J. Refrig.* **2017**, *82*, 348–365. [CrossRef]

11. Jribi, S.; Saha, B.B.; Koyama, S.; Chakraborty, A.; Ng, K.C. Study on activated carbon/HFO-1234ze(E) based adsorption cooling cycle. *Appl. Therm. Eng.* **2013**, *50*, 1570–1575. [CrossRef]

12. Fukuda, S.; Kondou, C.; Takata, N.; Koyama, S. Low GWP refrigerants R1234ze(E) and R1234ze(Z) for high temperature heat pumps. *Int. J. Refrig.* **2013**, *40*, 161–173. [CrossRef]

13. Le, V.L.; Feidt, M.; Kheiri, A.; Pelloux-Prayer, S. Performance optimization of low-temperature power generation by supercritical ORCs (organic Rankine cycles) using low GWP (global warming potential) working fluids. *Energy* **2014**, *67*, 513–526. [CrossRef]

14. Abdalla, G. Performance Characteristics of Automotive Air Conditioning System with Refrigerant R134a and Its Alternatives. *Int. J. Energy Power Eng.* **2015**, *4*, 168–177.

15. Kasaeian, A.B.; Daviran, S. Performance Analysis of Solar Combined Ejector-Vapor Compression Cycle Using Environmental Friendly Refrigerants. *IIUM Eng. J.* **2013**, *14*, 93–103. [CrossRef]

16. Direk, M.; Soylu, E. The effect of internal heat exchanger using R1234ze(E) as an alternative refrigerant in a mobile air-conditioning system. *J. Mech. Eng.* **2018**, *64*, 114–120.

17. Lemmon, E.W.; Bell, I.H.; Huber, M.L.; McLinden, M.O. *NIST Standard Reference Database 23: Reference Fluid Thermodynamic and Transport Properties-REFPROP*; Version 10.0; National Institute of Standards and Technolog: Gaithersburg, MA, USA, 2018.

18. Bolaji, B.O. Theoretical assessment of new low global warming potential refrigerant mixtures as eco-friendly alternatives in domestic refrigeration systems. *Sci. Afr.* **2020**, *10*, e00632. [CrossRef]

19. Zyczkowski, P.; Borowski, M.; Luczak, R.; Kuczera, Z.; Ptaszynski, B. Functional Equations for Calculating the Properties of Low-GWP R1234ze(E) Refrigerant. *Energies* **2020**, *13*, 3052. [CrossRef]

20. Bobbo, S.; Di Nicola, G.; Zilio, C.; Brown, J.S.; Fedele, L. Low GWP halocarbon refrigerants: A review of thermophysical properties. *Int. J. Refrig.* **2018**, *90*, 181–201. [CrossRef]

21. Liu, Y.; Wen, J.; Xu, P.; Khan, M.; Wang, S.; Tu, J. Numerical investigation on the condensation of R134a, R1234ze(E) and R450A in mini-channels. *Int. J. Refrig.* **2021**, *130*, 305–316. [CrossRef]

22. Tsatsaronis, G. Definitions and nomenclature in exergy analysis and exergoeconomics. *Energy* **2007**, *32*, 249–253. [CrossRef]

23. Bejan, A.; Tsatsaronis, G.; Moran, M.J. *Thermal Design and Optimization*; John Wiley and Sons: New York, NY, USA, 1996.

24. Kotas, T.J. *The Exergy Method of Thermal Power Plants Analysis*; Krieger Publ. Co.: Malabar, FL, USA, 1995.

25. Fazelpour, F.; Morosuk, T. Exergoeconomic analysis of carbon dioxide transcritical refrigeration machines. *Int. J. Refrig.* **2014**, *38*, 128–139. [CrossRef]

26. Ahmadzadeh, A.; Reza Salimpour, M.; Sedaghat, A. Thermal and exergoeconomic analysis of a novel solar driven combined power and ejector refrigeration (CPER) system. *Int. J. Refrig.* **2017**, *83*, 143–156. [CrossRef]

27. Mousavi, S.A.; Mehrpooya, M. A comprehensive exergy based evaluation on cascade absorption compression refrigeration system for low temperature applications—Exergy, exergoeconomic, and exergoenvironmental assessments. *J. Clean. Prod.* **2020**, *246*, 119005. [CrossRef]

28. Makhnatch, P.; Khodabandeh, R. The role of environmental metrics (GWP, TEWI, LCCP) in the selection of low GWP refrigerant. *Energy Procedia* **2014**, *61*, 2460–2463. [CrossRef]

29. IIR (International Institute of Refrigeration). *Guideline for Life Cycle Climate Performance*; International Institute of Refrigeration: Paris, France, 2016.

30. Troch, S.; Lee, H.; Hwang, Y.; Radermacher, R.; Harmonization of Life Cycle Climate Performance (LCCP) Methodology. *Int. J. Refrig. Air Cond. Conf.* **2016**, 1724. Available online: http://docs.lib.purdue.edu/iracc/1724 (accessed on 20 March 2022).

31. Lee, H.; Troch, S.; Hwang, Y.; Radermacher, R. LCCP evaluation on various vapor compression cycle options and low GWP refrigerants. *Int. J. Refrig.* **2016**, *70*, 128–137. [CrossRef]

32. Choi, S.; Oh, J.; Hwang, Y.; Lee, H. Life cycle climate performance evaluation (LCCP) on cooling and heating systems in South Korea. *Appl. Therm. Eng.* **2017**, *120*, 88–98. [CrossRef]